A Review of Convection Initiation and Motivation for IHOP_2002

TAMMY M. WECKWERTH AND DAVID B. PARSONS

Earth Observing Laboratory, National Center for Atmospheric Research, Boulder, Colorado*

(Manuscript received 26 August 2004, in final form 22 April 2005)

ABSTRACT

The International H_2O Project (IHOP_2002) included four complementary research components: quantitative precipitation forecasting, convection initiation, atmospheric boundary layer processes, and instrumentation. This special issue introductory paper will review the current state of knowledge on surface-forced convection initiation and then describe some of the outstanding issues in convection initiation that partially motivated IHOP_2002. Subsequent papers in this special issue will illustrate the value of combining varied and complementary datasets to study convection initiation in order to address the outstanding issues discussed in this paper and new questions that arose from IHOP_2002 observations.

The review will focus on convection initiation by boundaries that are prevalent in the U.S. southern Great Plains. Boundary layer circulations, which are sometimes precursors to deep convective development, are clearly observed by radar as reflectivity fine lines and/or convergence in Doppler velocity. The corresponding thermodynamic distribution, particularly the moisture field, is not as readily measured. During IHOP_2002, a variety of sensors capable of measuring atmospheric water vapor were brought together in an effort to sample the three-dimensional time-varying moisture field and determine its impact on forecasting convection initiation. The strategy included examining convection initiation with targeted observations aimed at sampling regions forecast to be ripe for initiation, primarily along frontal zones, drylines, and their mergers.

A key aspect of these investigations was the combination of varied moisture measurements with the detailed observations of the wind field, as presented in many of the subsequent papers in this issue. For example, the high-resolution measurements are being used to better understand the role of misocyclones on convection initiation. The analyses are starting to elucidate the value of new datasets, including satellite products and radar refractivity retrievals. Data assimilation studies using some of the state-of-the-art datasets from IHOP_2002 are already proving to be quite promising.

1. Introduction

Accurate, high-resolution, three-dimensional moisture measurements are critical, yet largely unavailable, for many atmospheric science applications (e.g., Weckwerth et al. 1999). For example, several national study groups (National Research Council 1998; Emanuel et al. 1995; Dabberdt and Schlatter 1996) have suggested that a critical factor limiting the prediction of convective precipitation is the measurement uncertainty in the high-resolution distribution of water vapor. Radiosondes, the traditional means of obtaining water vapor measurements, are insufficient because they provide vertical profile information at widely distributed locations, are typically only available twice a day, and sometimes contain significant errors and biases (e.g., Soden and Lanzante 1996; Guichard et al. 2000; Wang et al. 2002; Revercomb et al. 2003; Turner et al. 2003; Ciesielski et al. 2003). Additionally, there is a general absence of operational, scanning ground-based remote sensing systems for water vapor so that this variable is not sampled, for example, on the same spatial and temporal scales as radar measurements of precipitation. Satellite techniques show great promise to cover these spatial and temporal scales; however, current systems cannot obtain high-vertical-resolution water vapor measurements over land with high accuracy in the lower troposphere and can often be limited by extensive cloud cover.

* The National Center for Atmospheric Research is sponsored by the National Science Foundation.

Corresponding author address: Tammy M. Weckwerth, NCAR/EOL, P.O. Box 3000, Boulder, CO 80307-3000.
E-mail: tammy@ucar.edu

This water vapor measurement uncertainty was a primary justification for the International H_2O Project (IHOP_2002; Weckwerth et al. 2004). IHOP_2002 was actually born from the merger of several different efforts that had overlapping objectives related to water vapor: (i) United States Weather Research Program (USWRP)-funded research, led by D. Parsons and M. Hardesty, to examine the impact of improved water vapor measurements on the prediction of the initiation and evolution of convective systems, (ii) questions on the representativeness of soundings due to significant small-scale moisture variations (Weckwerth et al. 1996; Weckwerth 2000), (iii) a recommendation to conduct field campaigns for cross validation of water vapor measurement systems conceived at the 1998 National Center for Atmospheric Research (NCAR)/National Oceanic and Atmospheric Administration (NOAA) Water Vapor Workshop (Weckwerth et al. 1999), and (iv) the Thunderstorm Initiation Mobile Experiment (TIMEx), which could not be successful without demonstrated improvements in water vapor measurements. As a result IHOP_2002 had four complementary components:

(i) Quantitative precipitation forecasting (QPF), which aimed to determine the relative improvement in warm-season QPF skill from these enhanced moisture measurements. Warm-season convective rainfall, coupled with very low QPF skill (e.g., Uccellini et al. 1999; Fritsch and Carbone 2004), dramatically affects society in terms of flash floods, agriculture, transportation, and severe storm prediction.

(ii) Convection initiation (CI) process studies in which enhanced moisture measurements were obtained to better understand and predict the location and timing of new convection. This improved knowledge is an essential step in improving QPF skill.

(iii) The atmospheric boundary layer component, which examined surface heterogeneities and land-use differences to ascertain their relevance for CI and QPF.

(iv) The instrumentation component, which attempted to define the near-future optimal mix of remote and in situ moisture sensors to improve the prediction of warm-season rainfall.

While this special issue will focus on the CI component, exciting results utilizing IHOP_2002 special observations and/or modeling studies from the investigations outside of the CI research component are starting to appear in the literature (e.g., Wang et al. 2003; Weaver et al. 2004; Weckwerth et al. 2005; Ziegler et al. 2004).

The IHOP_2002 experimental domain (Fig. 1) was centered on the U.S. southern Great Plains (SGP). The regional variations in thermodynamic and dynamic characteristics over the SGP and how these variations relate to the storm environment have been known for some time (e.g., Miller 1959; Newton 1963; Carlson and Ludlam 1968; Carlson et al. 1983). For example, the characteristics of the IHOP_2002 region of study are known to vary significantly with longitude. In the eastern portion of the domain, the southerly flow is often very moist, having originated from the Gulf of Mexico and subsequently flowing over high soil moisture content. This moist boundary layer air is often capped with a strong inversion, creating a situation where the triggering of storms becomes critical. Because of substantial amounts of convective available potential energy (CAPE) in this moist flow, once the cap is broken, the ensuing thunderstorms may be severe. Near the center of the region, there are large mesoscale variations in water vapor, with changes often concentrated in a "dryline" where water vapor mixing ratio variations of several grams per kilogram can be concentrated in a few kilometers. Prior to the project, drylines were believed to be the primary surface-based forcing mechanism in the region for new convection forming as synoptic features approached (e.g., Rhea 1966). The local topographic variations are small and generally not critical to the triggering of convection, although the Texas Caprock area does exhibit an increased frequency of convection. The region has a nocturnal precipitation maximum (e.g., Wallace 1975). Recently a continental-scale organization has been noted with convection originating over the Rocky Mountains and subsequent clusters of heavy rainfall maintaining some coherency on their eastward propagation across the continent (Carbone et al. 2002).

This manuscript will first review convection initiation by boundaries prevalent in this SGP environment, including drylines, frontal regions, gust fronts, horizontal convective rolls, bores, and those due to land surface effects. A review of convection initiation by a broader assortment of boundaries can be found in Jorgensen and Weckwerth (2003). A discussion of some of the outstanding CI issues that were partially motivating factors for IHOP_2002 is presented in section 3. Conclusions are in section 4.

2. A review of convection initiation by boundaries and some key scientific questions

It has long been known that boundary layer convergence zones are sometimes precursors to convective development and organization. These low-level convergence zones often act to locally deepen the moist layer

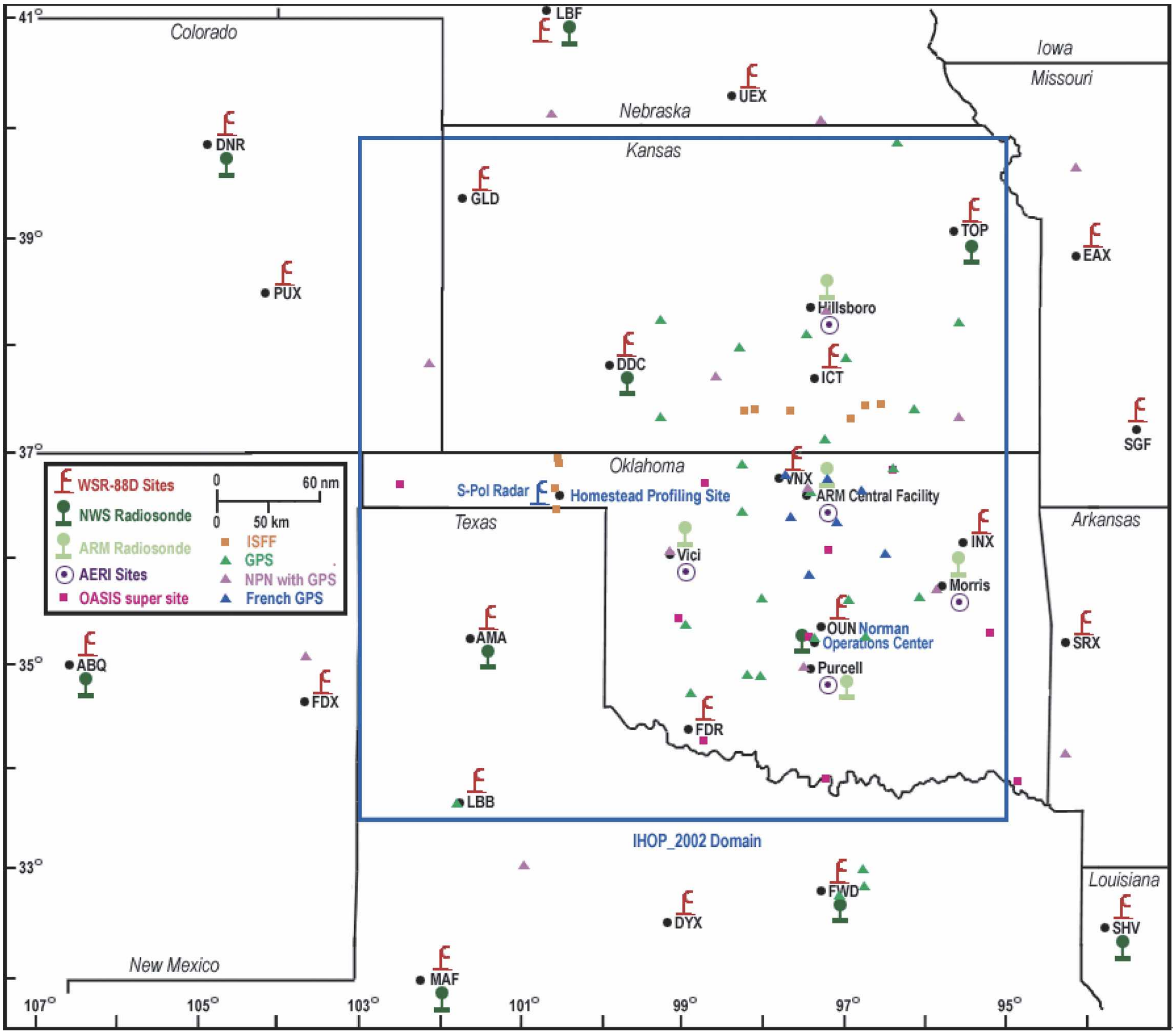

FIG. 1. Map illustrating the operational instrumentation within the IHOP_2002 domain. Instrumentation deployed for the project is also indicated. (From Weckwerth et al. 2004.)

and create conditions favorable for deep convection. Using surface data from the Thunderstorm Project in Florida, Byers and Braham (1949) observed these zones 20–30 min prior to the appearance of precipitation echoes. Subsequent studies also showed that surface mesonet anemometers detected convergence 15–90 min prior to the onset of convective rainfall (Ulanski and Garstang 1978; Garstang and Cooper 1981; Achtemeier 1983; Watson and Blanchard 1984). Purdom (1982) used satellite imagery to conclusively show that boundaries, as indicated by shallow linear cloud bands, occur prior to deep convective development. Following the work of Roberts and Rutledge (2003), Mecikalski and Bedka (2006), in this special issue, use advanced satellite products to further demonstrate the value of satellite imagery in forecasting convective development.

Using Doppler radar data in the Denver, Colorado, area, Wilson and Schreiber (1986) observed fine lines of enhanced reflectivity, which are indicative of boundary layer convergence zones. They showed that the apparently random geographic locations of first echoes were actually collocated with these fine lines. In fact, they found that 80% of thunderstorms in the Colorado Front Range were initiated within 10 km of boundary layer convergence zones. This was one of the early studies clearly illustrating the utility of radar data in detecting boundaries and identifying likely regions for convective development.

Purdom and Marcus (1982) used satellite imagery to determine that 73% of afternoon thunderstorms in the southeastern United States are triggered by the interactions of outflow boundaries. Wilson and Schreiber's (1986) radar study found that 71% of boundary collisions in the Denver area initiated thunderstorms. The resulting storms were relatively intense and often evolved into squall lines. Several detailed observational studies have subsequently shown that thunderstorms may initiate near the collision regions of two boundaries (e.g., Droegemeier and Wilhelmson 1985; Mahoney 1988; Carbone et al. 1990; Intrieri et al. 1990).

Boundary collisions, however, do not always produce convection (e.g., Wilson and Schreiber 1986; Stensrud and Maddox 1988). Kingsmill (1995) illustrated this in a case study of a sea-breeze front–gust front intersection. He noted that convection along the separate boundaries was more likely as the boundaries approached existing cumulus clouds. After the boundaries collided, the depth of the combined convergence zone decreased due to the effects of the relatively shallow sea-breeze front. The existence of preexisting small cumulus clouds was also previously shown to be a key ingredient for deep convective development with moving boundaries (e.g., Wilson and Mueller 1993; Hane et al. 1987; May 1999).

a. Factors controlling lifting and convection initiation at boundaries

Although satellite imagery often shows boundaries as thin cloud lines and the radar aptly identifies locations of boundaries through both Bragg scattering by strong thermodynamic gradients and Rayleigh scattering from insects in the precipitation-free clear air (e.g., Wilson et al. 1994), it is also necessary to have detailed thermodynamic measurements to obtain an accurate assessment of convective potential. Crook (1996) performed model sensitivity studies of convection initiation processes associated with convergence zones. He found that convection initiation is sensitive to the magnitude of the low-level vertical gradients of temperature and moisture. In particular, he noted that changing the magnitude of the vertical temperature gradient by only 1°C made the difference between no simulated storm and intense convection. The strength of the simulated storm varied significantly when the magnitude of the low-level moisture gradient changed by only 1 g kg^{-1}. These critical temperature and moisture variations are within the range of typical observational boundary layer variability (e.g., Weckwerth et al. 1996) providing a clear challenge for the forecasting of the initiation and intensity of convective rainfall. In a study relevant to this challenge, Fabry (2006), in this special issue, shows how the radar-derived near-surface refractivity field (Fabry et al. 1997; Fabry 2004; Weckwerth et al. 2005), which is a strong function of mixing ratio and less so of temperature, is related to convection initiation.

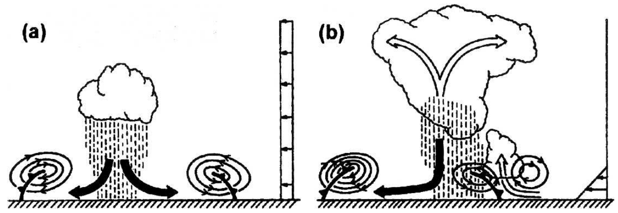

FIG. 2. Conceptual model of importance of low-level shear in the evolution of convection. (a) Without low-level shear, the cold-pool circulation inhibits deep vertical lifting and inhibits new convection. (b) With low-level shear countering the cold-pool circulation, new cells can be triggered. (From Rotunno et al. 1988.)

In addition to knowing the locations of boundaries and the detailed thermodynamics, the magnitude and depth of lifting at boundaries is also an important characteristic to storm initiation and maintenance. One aspect relevant to the lifting at boundaries is how the ambient wind shear profile interacts with the thermodynamics of the boundaries. Early numerical simulations (e.g., Moncrieff and Miller 1976; Droegemeier and Wilhelmson 1985; Rotunno et al. 1988; Parsons 1992) have proposed that the intensity, structure, and lifetime of storms and squall lines is dependent on the environmental wind profile and cold-pool strength, which control such factors as (i) the orientation of the updraft, (ii) strength and depth of ascent at the leading edge of the cold pool, and (iii) any differences between the motion of storms and the boundary that forced them. Figure 2 illustrates how the balance of horizontal vorticity, defined by the cold-pool strength and low-level shear, can lead to vertically oriented updrafts (e.g., Rotunno et al. 1988) with significantly stronger magnitudes (Parsons 1992). In some instances this balance may be more favorable after the collision of two boundaries (e.g., Carbone et al. 1990). This vorticity balance, however, may be a necessary but not a sufficient condition for deep convective development. Numerical simulations examining the intersections between boundary layer convergence lines by Lee et al. (1991) showed that storm initiation is sensitive to the amount of moisture, strength of convergence, and shear values. They found that increased low-level moisture creates stronger and taller modeled storms and that variations in boundary layer convergence affected the timing and character of the modeled storms while a threshold of shear above the boundary layer inhibited the convective development of the modeled storm.

Relatively less attention has been focused on applying these concepts to observational studies of the initial triggering of convection. Wilson and Megenhardt (1997) undertook an extensive examination of these concepts from ~30 days of radar data during the Convection and Precipitiation/Electrification (CaPE; e.g., Wakimoto and Lew 1993) experiment in Florida. The environment they investigated had low values of the vertical wind, and they found it useful to interpret their results in terms of the relative movement of storms and boundaries. Figure 3 shows favorable and unfavorable conditions for convection initiation and sustenance. In the top situation the gust front and storm steering level (~3 km wind) are similar, creating a favorable situation for convection. The unfavorable situation (bottom of Fig. 3) depicts steering-level winds that are opposite the gust front motion and this causes the storms to move away from their source of low-level convergence. The extent to which the concept of the relative movement of boundaries and developing convection controls storm initiation at boundaries in the capped, but highly unstable SGP environment, with the vertical shear being much larger than in Florida, is a question for IHOP_2002 research.

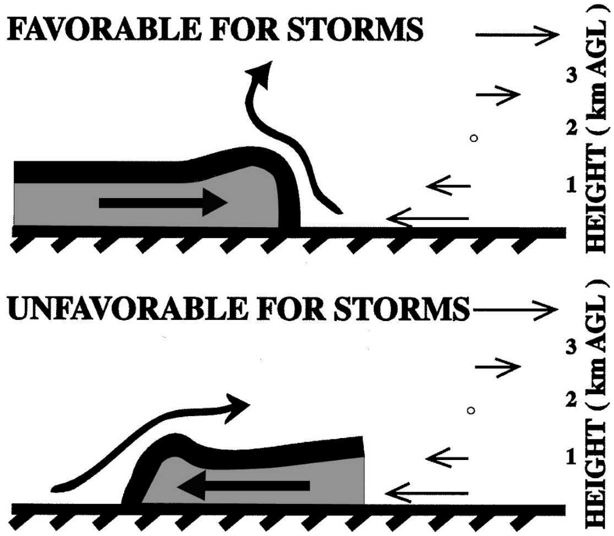

FIG. 3. Schematic illustration of dynamic conditions (top) favorable and (bottom) unfavorable for CI derived from observations in a relatively low shear environment. The wind vectors on the right represent the environmental wind profile, which is the same for both cases. The dark shading represents a density current, or boundary. The curved arrow ahead of the density current represents the updraft tilt. (From Wilson et al. 1998.)

A key question for IHOP_2002 will be to place the findings from this region concerning mechanisms for convection initiation at boundaries into the context of studies in other regions. For example, Raymond (1995) has argued that the tropical atmosphere over the western Pacific warm pool is typically quite near the threshold for the onset of convection. One may, therefore, hypothesize that the relative importance of ascent at boundaries could be diminished in such an environment in favor of the general energetics of the tropical boundary layer. The importance of deep, vertical ascent at cold pools in tropical squall-line systems may also be diminished (LeMone et al. 1998).

b. The role of three-dimensional variations in boundary structure and the initiation of convection

The original concepts of the importance of how vertical shear interacts with boundaries were in essence two-dimensional arguments, while boundaries in nature exhibit significant three-dimensional structure. Horizontal wave patterns thought to be driven by shearing instabilities have been observed along many boundary layer convergence zones (e.g., Hobbs and Persson 1982; McCarthy and Koch 1982; Carbone 1982, 1983; Parsons and Hobbs 1983; Mueller and Carbone 1987; Wakimoto and Wilson 1989; Wilson et al. 1992; Weckwerth and Wakimoto 1992; Kingsmill 1995). Detailed Doppler radar analyses by Carbone (1982) and Hobbs and Persson (1982) showed that these wave patterns produce alternating maxima of cyclonic vorticity and strong convergence in a precipitating cold front. The areas of vorticity are often apparent as regularly spaced, small-scale misocyclones. The misocyclones may be associated with inflections, or undulations, in the boundaries that are suspected to play a role in convection initiation (e.g., Kingsmill 1995; Lee and Wilhelmson 1997). The previous studies have focused on the kinematics and dynamics associated with the misocyclones, but IHOP_2002 affords the possibility of combining such measurements with the thermodynamics to obtain a complete picture of the impact of misocyclones and convergence areas on the moisture distribution along boundaries, as well as the relevance of these features to convection initiation. Two such studies examining these relationships among moisture, misocyclones, and CI are presented in this special issue by Murphey et al. (2006) and Markowski and Hannon (2006).

Convection initiation associated with some specific mesoscale boundary layer forcing mechanisms will subsequently be discussed. The boundary layer features to be highlighted include those that are prevalent in the IHOP_2002 domain: drylines, frontal zones, gust fronts, horizontal convective rolls, bores, and topographically induced boundaries. The finescale structures of IHOP_2002 boundaries and the adjacent boundary layer are examined by Karan and Knupp (2006). An overview of convection initiation by boundaries during

IHOP_2002 is presented in this issue by Wilson and Roberts (2006).

c. Drylines

The dryline is a zone of moisture gradient(s) separating the warm, moist air flowing northward from the Gulf of Mexico and the hot, dry air flowing eastward from the elevated terrain of the southwestern United States and northern Mexico. Another way to view the dryline is that it represents the intersection of the top of the moist layer to the east with the terrain that slopes upward to the west. The dryline typically ranges from 500 to 1000 km in length. Strong cross-dryline gradients in moisture occur on a scale of 1–20 km, which cannot be adequately sampled by the traditional sounding and surface networks (NSSP Staff 1963). These narrow dryline features can contain ascent of several meters per second (e.g., Parsons et al. 1991). Multiple moisture gradients frequently occur with "secondary" drylines located to the east of the stronger moisture gradient (e.g., Hane et al. 1993; Crawford and Bluestein 1997; Hane et al. 2001). Preferentially strong daytime boundary layer heating west of the dryline leads to more growth and more drying from entrainment of dry air from above, compared to the east side. This enhances the moisture differences across the dryline and enhances low-level convergence (Schaefer 1986).

The dryline has been the object of numerous investigations, perhaps because of its link to convective development. Nearly 40 yr ago, Rhea (1966) noted the frequency of convection initiation along the dryline during the spring and early summer months. Bluestein and Parker (1993) used 16 yr of radar data to identify modes of isolated severe storm development along the dryline. Critical conditions necessary for severe convective development include small values of convective inhibition (CIN), high CAPE values, and deep tropospheric wind shear. A three-dimensional modeling study showed that storms form along the dryline when moisture convergence, due to the thermally direct secondary dryline circulations, is sufficient to destabilize the local sounding to a state supportive of deep convection (Ziegler et al. 1997). Ziegler and Rasmussen (1998) summarized their case study in a schematic (Fig. 4) that shows the dryline relative to developing clouds and airflow streamlines. For development of deep convection it is essential that the moist boundary layer air parcels reach their lifting condensation level (LCL) and level of free convection (LFC) prior to leaving the mesoscale updraft zone.

Convection is seldom initiated uniformly along the entire length of the dryline. Determining the causes for the along-line variability has been a hot topic of research. Some potential explanations for preferred locations for convective development along the dryline include the following:

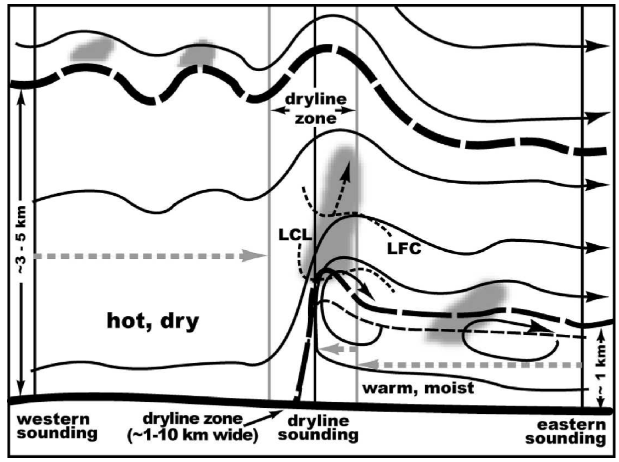

FIG. 4. Conceptual model of dryline environment during afternoon and early evening, showing dryline position relative to cumulus clouds and airflow streamlines. The lower thick dashed black line indicates the extent of the moist convective boundary layer, while the upper thick dashed black line denotes the deep, dry convective boundary layer west of the dryline and the elevated residual layer east of the dryline above the moist layer. The gray dashed line indicates the surface of zero westerly winds. The vertical streamline denotes a buoyantly accelerated cloudy air parcel trajectory. The vertical gray lines locate soundings discussed in their paper. (From Ziegler and Rasmussen 1998.)

- (i) Synoptic-scale dryline bulges (e.g., Tegtmeier 1974; Hane et al. 1997).
- (ii) Larger-scale features creating capped zones that sometimes trigger internal gravity waves that may then influence convective organization. McCarthy and Koch (1982) and Koch and McCarthy (1982) attributed along-dryline variability to zones of enhanced moisture convergence caused by dryline and gravity wave interactions. Sanders and Blanchard (1993) also found a relationship between dryline convection and gravity waves. They found that localized lifting of a capping inversion created waves that influenced convective development along a small sector of a western Kansas dryline.
- (iii) Mesoscale low pressure areas along the dryline. Bluestein et al. (1988) observed localized differences in low-level diabatic heating, which led to pressure decreases in the dry air that locally enhanced low-level convergence and led to convection initiation.
- (iv) Boundary layer circulations intersecting the dryline. Hane et al. (1997) observed the formation of a cloud line in the dry air west of a dryline. The cloud line apparently formed owing to landscape

and land-use differences. The intersection of the cloud line with the dryline produced enhanced convergence that led to development of tornadic storms in northwest Oklahoma. In another case, Hane et al. (2002) observed convection initiation at the intersection of a cloud line with a rapidly advancing dryline. The cloud line developed over a region that had received the heaviest rainfall during the previous night. Along another section of this dryline, no storms formed owing to cooler boundary layer air resulting from reduced daytime heating over an area that had received significant rainfall during the previous night. Along a third section of the dryline, deep convection developed due to enhanced convergence from backed winds in locally moist air in response to decreased pressure in the warm air to the northwest. Atkins et al. (1998) found that variations in cloud development along the dryline were due to intersections with horizontal convective rolls. They observed reflectivity maxima and sometimes cloud formation at the intersection points.

The measurements during IHOP_2002 have the capacity and resolution to help us further understand the dryline circulation and establish the role of the dryline in the initiation of convection. From the early stages of IHOP_2002 planning, the dryline was a likely target for the CI component. It was an appealing boundary to study because of its frequency in the region, slow propagation speed, and its perceived likelihood of initiating convection. In fact the majority of the IHOP_2002 CI missions were directed at drylines or intersections between drylines and other boundaries. Most of those missions resulted in null CI cases. Furthermore, Wilson and Roberts (2006) show that dryline circulations were not the leading cause of CI in the summer of 2002. Detailed analyses of drylines with (Wakimoto et al. 2006; Murphey et al. 2006) and without (Weiss et al. 2006; Demoz et al. 2006; Cai et al. 2006) convection initiation are included in this special issue.

d. Frontal boundaries and frontal–dryline mergers

Convection initiation along cold fronts has been noted for some time (e.g., Koch 1984; Dorien et al. 1988; Koch and Kocin 1991). Previous research has illustrated how balanced secondary circulations associated with cold fronts produce ascent over mesoscale areas (~50 km) that create an environment more favorable to the initiation of convection (e.g., Shapiro 1981, 1982; Trier et al. 1991). The balanced ascent may act to deepen the low-level moisture in advance of the cold air to produce an environment favorable for CI. In addition, strong local ascent (several meters per second) within 1–2 km of the leading edge of cold fronts (e.g., Shapiro et al. 1985) can trigger convection along fronts as the fronts move into a more favorable environment.

Cold fronts and drylines may act in concert (i.e., frontal–dryline mergers; Shapiro 1982) to produce severe weather (e.g., Koch and McCarthy 1982; Ogura 1982; Schaefer 1986; Keyser and Shapiro 1986; Doswell 1987; Parsons et al. 1991, 2000; Hane et al. 1993; Neiman and Wakimoto 1999). It has been shown that the approach of a cold front toward a dryline can induce frontogenetical circulations along the dryline that enhance the vertical velocities and initiate convection (Koch and McCarthy 1982). Additionally as the boundaries merge, the vertical motions associated with the two boundaries are in phase and the parcels may more readily reach the LFC (e.g., Neiman and Wakimoto 1999).

Convection often initiates at the "triple point," which is the intersection region between a baroclinic boundary and dryline (e.g., Bluestein et al. 1990; Reed and Albright 1997; Weiss and Bluestein 2002). Figure 5 schematically illustrates the flow field associated with the three air masses and the expected preferred region of deep convection near the triple point. Bluestein et al. (1990) observed locally enhanced convergence and a local deepening of the moist layer, resulting in cumulus congestus and small cumulonimbus forming at the triple point. In a case study of a dryline–gust front intersection, Weiss and Bluestein (2002) found that convection was initiated at a dryline–gust front intersection in one of two ways. First, the approaching gust front enhanced the upwelling part of the dryline circulation, thereby creating a more favorable region for convection initiation. Second, the gust front and its associated deep updrafts lifted air parcels to their LCL prior to the interaction of the two boundaries, priming the intersection region for deep convection.

Convection does not always develop at frontal–dryline merger or intersection locations, however. In a severe squall-line case study, initiation did not occur at the intersection between a cold front and dryline. Koch and Clark (1999) observed the development of a gravity current at the leading edge of the cold front. This produced a bore that propagated ahead on the surface-based stable layer and triggered a severe squall line along the part of the front that produced the prefrontal bore.

Frontal boundaries and their interactions with drylines were often targeted during the project. IHOP_2002 frontal boundaries mainly included cold

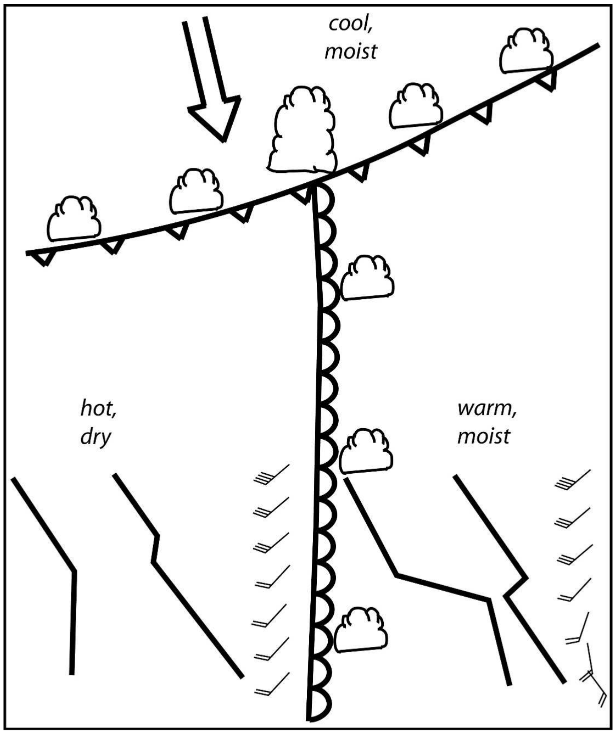

FIG. 5. Conceptual model of cold front–dryline intersection. The baroclinic boundary is indicated by a barbed line while the dryline is depicted with half circles. Large arrow depicts general flow field. Schematic clouds show the relative size and frequency along the dryline and cold front in contrast to deeper convective development at the triple point. As presented in Weiss and Bluestein (2002), typical soundings on either side of the dryline are shown.

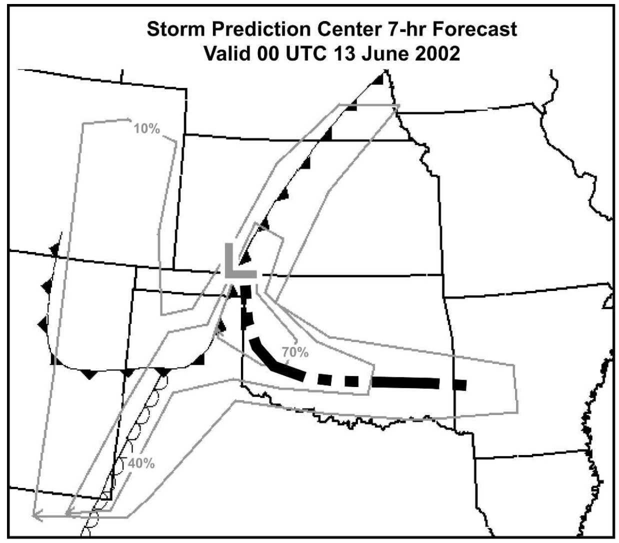

FIG. 6. Sample SPC boundary and CI forecast product valid on 12 Jun 2002. The barbed boundary indicates a cold front; the half-circle boundary indicates the dryline; and the dotted–dashed line indicates an outflow boundary. The likelihood of convection is indicated by percentages for various regions.

fronts and stationary fronts, but, additionally, warm fronts. These synoptic-scale fronts were optimal targets due to their predictability 1–2 days in advance of the event and likelihood of initiating storms. An example Storm Prediction Center (SPC) 1-day (i.e., the same afternoon/evening) boundary and CI forecast is shown in Fig. 6. These forecast locations of boundaries and likelihood of CI were highly valued tools in defining which of the IHOP_2002 missions should be called for day 2 (i.e., the subsequent day), as well as for planning the current day-1 CI missions. Some of the IHOP_2002 CI cold-frontal missions had to be aborted because the ground-based mobile armada could not collect good quality data when the boundary observed was moving faster than 5–10 m s^{-1}. Many IHOP_2002 missions focused on triple points between cold fronts and drylines. Triple points were readily forecast and were straightforward to detect with ground-based and airborne in situ instrumentation.

IHOP_2002 measurements are well suited to the examination of several issues concerning fronts and convection initiation including the relative role of secondary circulations in preconditioning, whether the strong local ascent sometimes observed in high-resolution modeling and observations is a common phenomena and the role of alongfront variations in lifting and/or thermodynamics. A detailed analysis of a cold-frontal boundary is presented in Geerts and Damiani (2006) in this special issue. One null convection initiation case study along a cold front on 10 June 2002 is presented by Arnott et al. (2006). Two triple-point CI case studies are presented in this special issue (Wakimoto et al. 2006; Markowski et al. 2006).

e. Gust fronts

The rain-cooled downdraft air of thunderstorms creates a low-level cold pool characterized by density differences between it and the ambient air. Gust fronts are the leading edges of such cold-air outflows. These density currents have been studied using tower data (e.g., Charba 1974; Goff 1976), Doppler radar data (e.g., Wakimoto 1982; Mueller and Carbone 1987), wind profilers with the radio acoustic sounding system (RASS; May 1999), and numerical modeling (e.g., Seitter 1986; Droegemeier and Wilhelmson 1985). Of all the boundaries examined in the high plains by Wilson and Schreiber (1986), gust fronts were most often associated with convection initiation.

Waves are often produced along gust fronts and the interactions between the waves and the outflow boundary have been shown to influence convective development (e.g., May 1999). Utilizing radar, surface stations, and radiosondes, Carbone et al. (1990) illustrated that vertices in a line-echo wave pattern (a series of 80–150-km-long arcs in radar reflectivity) along a gust front were the preferred locations for surface convergence and for convective development. Deep convection occurred along the gust front only after interaction with the dryline and/or low-level jet. This outflow boundary first propagated as a density current and evolved toward an internal undular bore. Dual-Doppler radar analyses also showed waves generated atop the cold-air outflow (e.g., Mueller and Carbone 1987; Weckwerth and Wakimoto 1992). Weckwerth and Wakimoto (1992) found that internal gravity waves and Kelvin–Helmholtz waves influenced the initiation and organization of small convective cells generated at the gust front.

Proper representation of cold pools in numerical models has been shown to be essential for an accurate prediction of deep convective events, especially when the synoptic-scale forcing is not strong (e.g., Stensrud and Fritsch 1994; Stensrud et al. 1999). Thus simulations must either explicitly resolve cold-pool circulations or parameterize their effects.

Newly generated gust fronts were not directly targeted during IHOP_2002 CI missions due to their high propagation speeds and the inability to forecast their existence and location for timely deployment of mobile observing platforms. There were, however, some missions that examined old outflow boundaries and their interactions with boundary layer circulations, internal gravity waves, and drylines (e.g., Markowski et al. 2006).

f. Horizontal convective rolls

Horizontal convective rolls are a common form of boundary layer convection manifested as counterrotating vortices about the horizontally oriented axis. Clouds often form atop the updraft branches of rolls (e.g., Kuettner 1959, 1971; LeMone and Pennell 1976; Christian and Wakimoto 1989). Rolls and cloud streets can extend hundreds of kilometers and last several hours. The conditions necessary for roll development and maintenance are surface-layer heat flux, some minimal low-level wind shear, and somewhat uniform surface characteristics (e.g., LeMone 1973; Grossman 1982; Weckwerth et al. 1997). Rolls commonly occurred during IHOP_2002 and often intersected larger synoptic-scale boundaries.

Intersection regions between convergence zones and horizontal convective roll updraft zones are often preferred locations for enhanced updrafts and cloud formation (e.g., Kessinger and Mueller 1991; Wilson et al. 1992). For example, intersections between the Denver convergence zone and rolls were observed (Wilson et al. 1992) and simulated (Crook et al. 1991) to be optimal locations for convective development. In a case study using Doppler radars, aircraft, mesonets, soundings, and a 2D numerical model, Fankhauser et al. (1995) found that while sea-breeze front–horizontal convective roll intersections were insufficient to initiate deep convection, the interactions between the same rolls with a thunderstorm outflow did trigger storms.

In other studies of the sea-breeze front intersecting horizontal convective rolls, enhanced updrafts and clouds were observed due to increased lifting at the intersection regions (Wakimoto and Atkins 1994; Atkins et al. 1995). Two detailed case studies (Atkins et al. 1995) and numerical simulations (Dailey and Fovell 1999; Fovell and Dailey 2001) compared rolls normal to and parallel to the sea-breeze front. When the rolls intersected the front at a large angle, the roll circulations were tilted upward by the frontal updraft, thereby creating stronger, deeper updrafts and deeper convection at the intersection zones. Furthermore, clouds that occurred at periodic intervals along the rolls intensified as the sea-breeze front intercepted them. In contrast, when the rolls were nearly parallel to the boundary, the front merged with the rolls, thereby strengthening the front when like-sign vortices interacted. Clouds formed along the intensified portions of the front and at the locations of periodic enhancements of the rolls that were present prior to the merger. It has also been suggested that the interactions of internal gravity waves propagating along the inversion layer at the top of the boundary layer with roll circulations within the boundary layer can initiate deep convection (Balaji and Clark 1988). Trier et al. (1991) found that deep convection was initiated from shallow roll clouds due to the destabilizing influence of the secondary circulations associated with an approaching cold front.

A numerical study illustrated the production of shear-parallel precipitating convection from roll vortices (Soong and Tao 1984). In a study of 13 days in east-central Florida during the CaPE project, it was shown that rolls are capable of initiating deep convection in the absence of intersections with another boundary (Weckwerth 2000). This study noted that roll updraft measurements (in contrast to general boundary layer measurements) are necessary to ascertain whether the environment is suitable for deep convective development. Previous studies have also shown the degree of moisture variability associated with horizontal roll circulations (e.g., LeMone and Pennell 1976;

Reinking et al. 1981). The roll updraft branches force moist, near-surface air upward into the boundary layer while the roll downdraft branches bring downward dry air from near the inversion level (e.g., Weckwerth et al. 1996). Since clouds and thunderstorms form atop roll updraft branches, it is essential that this updraft air be sampled to obtain an upper limit of the potential for deep moist convection (Fig. 7). Because of mixing, it is the upper limit sampled in the roll updraft branches that impacts storms larger than the roll scale. For updrafts that extend across two–three rolls, the moisture mass flux ingested into the storm would be greater than the boundary layer average and less than the value in the roll updraft (LeMone et al. 1988).

Although rolls were common during IHOP_2002, they were not observed to initiate convection on their own accord. There are, however, several cases in which rolls intersected larger mesoscale boundaries within the IHOP_2002 intensive observational regions and those intersections are sampled in great detail. Two of these studies include Markowski et al. (2006) and Arnott et al. (2006).

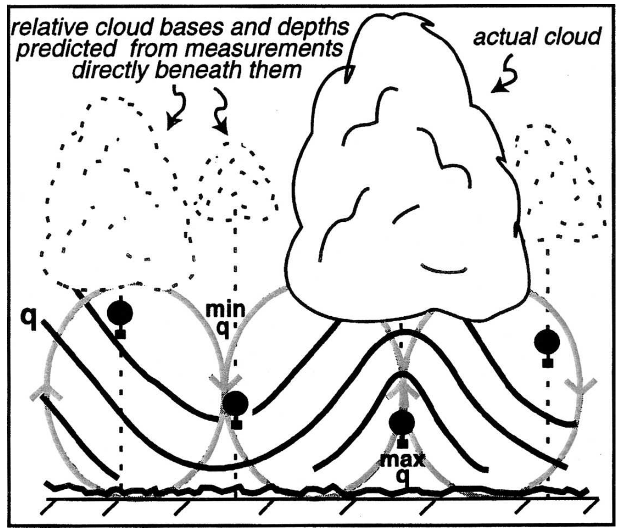

FIG. 7. Schematic diagram showing boundary layer moisture contours (solid black lines) associated with horizontal convective rolls (gray circulations). Actual cloud bases and depths atop roll updraft branches are shown by the solid cloud. Dashed clouds represent the relative cloud bases and depths expected if stability parameters were estimated from boundary layer moisture values directly beneath those clouds. (From Weckwerth et al. 1996.)

g. Undular bores and solitary waves

One of the surprising observations during IHOP_2002 was the multitude of bore events in the region. In the presence of shear, undular bores or solitary waves may be induced at or ahead of various atmospheric density currents (e.g., Haase and Smith 1984; Carbone et al. 1990; Koch et al. 1991; Kruse and Johnson 1995; Locatelli et al. 1998; Koch and Clark 1999) or at the collision of such boundaries (e.g., Wakimoto and Kingsmill 1995; Kingsmill and Crook 2003). Bores cause a "permanent" displacement of a layer aloft while atmospheric solitary waves occur when a layer is displaced upward and then returns back to its original height. However, since Christie et al. (1979) and Skyllingstad (1991) clearly make the case that under proper conditions bores can evolve into solitary wave systems, solitary wave events are included in this bore discussion.

Early investigators (e.g., Tepper 1950; Abdul 1955) were intrigued by observations of strong wave-related surface pressure perturbations and proposed that vertical motions arising from low-level gravity wave disturbances could initiate convective storms over the central plains. Since the early studies there have been numerous case study analyses showing solitary waves and borelike disturbances (e.g., Shreffler and Binkowski 1981; Doviak and Ge 1984; Fulton et al. 1990; Doviak et al. 1991; Koch et al. 1991; Mahapatra et al. 1991) and associated examples of convection initiation in which these wave events played a role (Carbone et al. 1990; Karyampudi et al. 1995; Koch and Clark 1999; Koch et al. 2001; Locatelli et al. 2002; Kingsmill and Crook 2003). Doviak et al. (1991) argue that these events "might be a commonly occurring feature in the neighborhood of thunderstorms whenever suitable atmospheric stratification exists and sources are active" and indeed borelike disturbances have commonly been observed (for a review see Menhofer et al. 1997). However, the observational investigations of solitary waves/bore events over the SGP have been primarily limited to individual case studies often using detailed measurements taken at a single location.

The IHOP_2002 measurements are well suited to a more systematic investigation of bore events, particularly because of the complete radar coverage afforded by the radar composites and nocturnal research flights with the water vapor differential absorption lidar (DIAL) systems. The measurements from aircraft and the fixed remote sensing systems together allow unprecedented investigations into the bore structure and evolution. The depth of the bore circulation, and the moisture convergence associated with it, are unknown quantities that may influence convection initiation, maintenance, and organization associated with bores. While detailed bore studies will appear in the subsequent literature, Wilson and Roberts (2006) show statistics on the frequency of bore-related IHOP_2002 convection initiation in this issue.

h. Topographic and land surface effects

Numerous studies have illustrated the importance of regional gradients in surface characteristics for accurately predicting the onset of convection (e.g., Anthes et al. 1982; Benjamin and Carlson 1986; Benjamin 1986; Lanicci et al. 1987; Sun and Wu 1992). Segal and Arritt (1992) showed that significant spatial heterogeneities in daytime sensible heat flux are common over land on a variety of scales. These heterogeneities can lead to thermally induced circulations due to land-use variations, contrasts in soil moisture owing to antecedent precipitation, natural landform variations, contrasts in cloudiness or contrasts in snow cover. Modeling studies have shown circulations with intensities comparable to the sea breeze, while observations suggest reduced intensity compared to the model results. On a regional scale, these heterogeneities are also linked to the intensity of the dryline.

Knupp et al. (1998) observed the initiation of a mesoscale convective system (MCS) within a synoptically benign environment. They found that convection initiation resulted from preexisting cloud streets and variability in surface heat flux, which produced solenoidally driven mesoscale circulations. The heat flux variations were due to cloud shading and antecedent rainfall. They determined that it is essential for mesoscale models to include an accurate representation of the atmospheric boundary layer and associated surface flux variables if they are to produce an accurate prediction of convective development. Nowcasting the initiation of convection from such subtle boundaries is quite challenging.

The importance of soil moisture, surface measurements, and land surface variations in forecasting convection initiation in the IHOP_2002 region are addressed in this special issue by Holt et al. (2006) and Childs et al. (2006).

3. Motivation for IHOP_2002 convection initiation observing strategies

Many of the scientific motivating factors for the IHOP_2002 CI component are tied to the primary outstanding issues in understanding CI over the SGP. As reviewed in section 2, it is well known that CI is commonly triggered by low-level convergence zones, but it is not known which boundaries will be successful in initiating storms or where along the boundaries the storms will form or when the convection will commence. Some of the IHOP_2002 research activities were thus motivated by the relatively recent technological advances to obtain some of the following measurements.

a. Targeted observations

The SGP is a region with high instability, thus allowing for severe storms, but also large inhibition to initiation, thus requiring substantial forcing to initiate storms. An important forecast objective with significant societal relevance is the prediction of exactly when and where this intense convection will develop. Thus IHOP_2002 adopted the strategy of targeting an extensive collection of airborne and ground-based observing systems near boundaries deemed likely to trigger deep, moist convection. This armada included mobile mesonets, mobile Doppler radars, mobile profilers, mobile sounding systems, and six remote and in situ sensing aircraft (Weckwerth et al. 2004). The targeted observations are essential components of numerous papers in this issue (e.g., Wakimoto et al. 2006; Geerts and Damiani 2006; Murphey et al. 2006; Weiss et al. 2006; Cai et al. 2006; Markowski and Hannon 2006; Markowski et al. 2006; Demoz et al. 2006; Arnott et al. 2006; Karan and Knupp 2006). A key question for future research is whether the addition of these targeted measurements will improve the prediction of convection initiation and thus the accuracy of quantitative precipitation forecasts when these observations are assimilated into next-generation, high-resolution forecast models. While such an approach of targeting measurements in regions of forecast uncertainty in order to improve initial conditions for model forecasts is novel for warm-season convection initiation, the theoretical concept of targeting driven by defining model uncertainties in forecast models is well established for synpotic-scale numerical weather prediction (e.g., Langland et al. 1999).

b. Combining thermodynamic and kinematic measurements

Previous studies have shown the sensitivity of CI to local lifting, vertical shear, and the thermodynamics of the lower troposphere (e.g., Rotunno et al. 1988; Carbone et al. 1990, 2000; Lee et al. 1991; Laird et al. 1995; Ziegler and Rasmussen 1998; Hane et al. 2002). Most past observational studies have utilized ground-based and/or airborne Doppler radar measurements to study boundaries through knowledge of the kinematics of the wind field. These studies were sometimes supplemented with airborne in situ measurements or a few mobile sounding sites. IHOP_2002 attempted to map the thermodynamics associated with these boundaries to supplement the approach of measuring the kinematics of these features. The strategy included extensive use of dropsondes, fixed and mobile surface stations, ground-based and airborne water vapor lidars, and radar refractivity (Weckwerth et al. 2004). The project concentrated on water vapor, which is consistent with the studies that quote the current uncertainty and importance of water vapor to the prediction of convection (e.g., Emanuel et al. 1995; Dabberdt and Schlatter 1996; Crook 1996). Components of the extensive assortment of IHOP_2002 water vapor sensors are used by all papers in this special issue. The combination of previously deployed kinematic measurement approaches, such as by mobile Doppler radar and wind profilers, with moisture measurements to further understand convection initiation and boundary layer processes, was a key motivating factor for the experiment.

c. Preconvective, high-resolution measurements

One aspect of CI is that it is a cumulus-scale process such that a boundary layer parcel must overcome static stability through forced ascent. Typically past studies have lacked three-dimensional high-resolution thermodynamic, particularly water vapor, and kinematic measurements on small cumulus scales at multiple boundaries and boundary types. Thus the IHOP_2002 armada of mobile sensors was deployed to sample the high-resolution boundary layer kinematics and thermodynamics prior to CI. These high-resolution measurements document preconvective processes in unprecedented detail (e.g., Karan and Knupp 2006; Wakimoto et al. 2006; Geerts and Damiani 2006; Murphey et al. 2006; Weiss et al. 2006; Cai et al. 2006; Markowski and Hannon 2006; Markowski et al. 2006; Demoz et al. 2006; Arnott et al. 2006). Encouraging data assimilation studies using water vapor DIAL measurements are presented in Wulfmeyer et al. (2006). While mobile radars, profilers, and surface armadas have been previously deployed, IHOP_2002 pushed the envelope on the number and utilization of such systems in high-resolution studies.

d. Multiscale measurements

IHOP_2002 was designed to capture many of the multiscale aspects of atmospheric and surface characteristics that influence where and when convection first forms. This strategy had several aspects. First, an effort was made to combine the operational and research radar datasets at the highest resolution possible into a single composite. Another aspect was to have CI flight plans designed to focus both locally on the boundaries and on the mesoscale structure of the cross-boundary environment utilizing both airborne remote sensors and dropsondes. Finally, the location of the IHOP_2002 domain allowed the project's observations to be placed within the existing operational and research measurement arrays. In the case of the National Weather Service sounding network, the experimental design included enhancing the number of soundings during periods of interest over a broad area. With this measurement strategy, the intent was to capture local ascent and circulations at the boundaries, capture the effects of any secondary, balanced circulations in preconditioning the environment, and to place these measurements in the synoptic context.

To place this multiscale concept in historical prospective, early studies recognized the large-scale influence, such as the pioneering climatological study by Rhea (1966) noting the link between convection initiation over this region and approaching synoptic disturbances. Thus, many of the early studies of outbreaks of convection over this region clearly demonstrated the importance of mesoscale and regional variations in inversion strength, convective instability, and depth of the moisture in controlling where convection formed. These mesoscale and synpotic variations were, in turn, proposed to be produced by the atmospheric response to variations in surface characteristics (e.g., Lanicci et al. 1987), and the ageostrophic (e.g., Uccellini and Johnson 1979) and balanced secondary circulations (Shapiro 1981) aloft associated with jet streaks, fronts, elevated mixed layers, and other synoptic-scale flow features.

Many excellent and focused field efforts took place over this region to look at the role of larger-scale flows in initiating convection. For, example, the focus on the role of mesoscale variations in forcing convection together with the newly developing tool of mesoscale modeling led to a large community field effort in 1979 called the Severe Environmental Storms and Mesoscale Experiment [SESAME; see Hill et al. (1979) for more information on this project]. Comparison of these experiments suggests that SESAME had a much more extensive mesoscale-synoptic radiosonde network, while advancing technology allowed IHOP_2002 to focus more on local measurements. The need for a more extensive research radiosonde network for SESAME was probably due to the improvements in the capabilities of forecast models, assimilation systems, and operational measurements (e.g., satellite sensing, profiling networks, and flight-level data). Many papers in this special issue utilize the multiscale observations obtained during IHOP_2002 (e.g., Wakimoto et al. 2006; Murphey et al. 2006; Cai et al. 2006; Markowski et al. 2006; Demoz et al. 2006).

e. Model evaluations

The current uncertainties in the prediction of convective rainfall, in general, and CI, in particular, and the importance of prediction of CI at boundaries over the SGP led to the examination of how well numerical operational and high-resolution research models predict the onset of convection. IHOP_2002 included a significant modeling component that allowed researchers to investigate convective triggering in these models and to evaluate the model prediction against detailed observations. The detailed nature of the observations, plus an extensive use of satellite and ground-based sounders, will allow researchers to have a physical framework for model evaluation. In this issue, Holt et al. (2006) discuss the sensitivities of low-level thermodynamics and fluxes, the dryline, and convection in the Coupled Ocean/Atmosphere Mesoscale Prediction System (COAMPS) model to changes in land surface models. Xue and Martin (2006a,b) present an evaluation of a high-resolution model in forecasting a triple-point initiation event. Martin and Xue (2006) perform sensitivity analysis of convection using an ensemble of over 12 000 mesoscale model forecasts. Wilson and Roberts (2006) address the performance of the Rapid Update Cycle (RUC) operational model for convection initiation events.

4. Summary

The CI component of IHOP_2002 was undertaken to better understand CI processes and their link to precipitation in the SGP. The papers in this special issue show detailed analyses of the impact of numerous boundary types, including drylines, outflow boundaries, cold fronts, horizontal convective rolls, topographically induced boundaries, and bores on CI. While the papers in this special issue have advanced the understanding of CI over the SGP, in some regards these investigations only represent the first step in using this rich dataset. For example, further work is needed to extend and synthesize these studies and determine the extent to which IHOP_2002 represents a typical year over the region. Also, improved knowledge of the triggering of storms in this region can and should be utilized to test and improve the treatment of convective triggering in numerical models. Another question related to numerical studies is determining whether assimilation of the targeted local measurements will improve the forecast of CI. In addition, further studies are needed to determine the extent to which convection initiation is predictable given the current and future observing networks and what factors limit the predictability of CI. IHOP_2002 showed that elevated convection (without surface-based forcing) was quite frequent. The causes of this elevated convection initiation requires better understanding before significant improvements in forecasting capabilities can be achieved.

The IHOP_2002 program will be complementary to two other field campaigns. The conditions in the SGP region are characterized by large convective instability with a strong capping inversion wherein the triggering of storms is essential. The local orographic variations are small and generally not critical to the triggering of convection. Another similar field effort is the Convective Storms Initiation Project (CSIP), which will took place over the southern portions of the United Kingdom in summer 2005. The meteorology and terrain offer a significant contrast to IHOP_2002. The goals of CSIP are to better understand and predict convection initiation of heavy precipitation events. The other related upcoming project is the Convective and Orographically Induced Precipitation Study (COPS), planned for the low-mountain region of southwestern Germany/eastern France in summer 2007. The environment will be more marine than IHOP_2002 but more continental than CSIP. From IHOP_2002 to CSIP to COPS, there will be a gradual transition to more complex terrain. While these three experiments have similar goals, there are different physics and stability conditions with each of them. Together these experiments will greatly improve the understanding of CI and QPF over a broad flow regime. A subsequent challenge for researchers will be to place the convective initiation findings from IHOP_2002, CSIP, and COPS into the broader context of scientific understanding of convection in other locations and to improve model predictions of the onset of convection.

IHOP_2002 has contributed a vastly rich dataset to better understand CI processes. This special issue will present some of the first results of the analyses. Numerous further studies will be presented in later issues and various fora.

Acknowledgments. Much of this research was funded through the NCAR/United States Weather Research Program. Strong support and commitments from NCAR/ATD (D. Carslon) and NSF (S. Nelson) were critical to realize the scope and magnitude of IHOP_2002. Some of this work is based upon research supported by the National Science Foundation under Grant 0208651.

Gratitude is bestowed upon Conrad Ziegler and David Kingsmill for creating the original IHOP_2002 CI hypotheses summary. Critical reviews of this manuscript by Rita Roberts, Jim Wilson, Peggy LeMone, and Kevin Knupp led to substantial improvements. The concept for Fig. 5 was conceived through discussions with J. Wilson. C. Pettet made the figure. Thanks are given to J. Gerleman who recreated Fig. 4.

REFERENCES

Abdul, J. A., 1955: The atmospheric solitary wave. *Bull. Amer. Meteor. Soc.,* **36,** 511–518.

Achtemeier, G. L., 1983: The relationship between the surface wind field and convective precipitation over the St. Louis area. *J. Climate Appl. Meteor.,* **22,** 982–999.

Anthes, R. A., Y.-H. Kuo, S. G. Benjamin, and Y.-F. Li, 1982: The evolution of the mesoscale environment of severe local storms: Preliminary modeling results. *Mon. Wea. Rev.,* **110,** 1187–1213.

Arnott, N. R., Y. P. Richardson, J. M. Wurman and E. M. Rasmussen, 2006: Relationship between a weakening cold front, misocyclones, and cloud development on 10 June 2002 during IHOP. *Mon Wea. Rev.,* **134,** 311–335.

Atkins, N. T., R. M. Wakimoto, and T. M. Weckwerth, 1995: Observations of the sea-breeze front during CaPE. Part II: Dual-Doppler and aircraft analysis. *Mon. Wea. Rev.,* **123,** 944–969.

——, ——, and C. L. Ziegler, 1998: Observations of the finescale structure of a dryline during VORTEX 95. *Mon. Wea. Rev.,* **126,** 525–550.

Balaji, V., and T. L. Clark, 1988: Scale selection in locally forced convective fields and the initiation of deep cumulus. *J. Atmos. Sci.,* **45,** 3188–3211.

Benjamin, S. G., 1986: Some effects of surface heating and topography on the regional severe storm environment. Part II: Two-dimensional idealized experiments. *Mon. Wea. Rev.,* **114,** 330–343.

——, and T. N. Carlson, 1986: Some effects of surface heating and topography on the regional severe storm environment. Part I: Three-dimensional simulations. *Mon. Wea. Rev.,* **114,** 307–329.

Bluestein, H. B., and S. S. Parker, 1993: Modes of isolated, severe convective storm formation along the dryline. *Mon. Wea. Rev.,* **121,** 1354–1372.

——, E. W. McCaul Jr., G. P. Byrd, and G. R. Woodall, 1988: Mobile sounding observations of a tornadic storm near the dryline: The Canadian, Texas, storm of 7 May 1986. *Mon. Wea. Rev.,* **116,** 1790–1804.

——, ——, ——, R. L. Walko, and R. P. Davies-Jones, 1990: An observational study of splitting convective clouds. *Mon. Wea. Rev.,* **118,** 1359–1370.

Byers, H. R., and R. R. Braham Jr., 1949: *The Thunderstorm*. U.S. Government Printing Office, 287 pp.

Cai, H., W.-C. Lee, T. M. Weckwerth, C. Flamant, and H. V. Murphey, 2006: Observations of the 11 June dryline during IHOP_2002—A null case for convective initiation. *Mon Wea. Rev.,* **134,** 336–354.

Carbone, R. E., 1982: A severe frontal rainband. Part I: Storm-wide hydrodynamic structure. *J. Atmos. Sci.,* **39,** 258–279.

——, 1983: A severe frontal rainband. Part II: Tornado parent vortex circulation. *J. Atmos. Sci.,* **40,** 2639–2654.

——, J. W. Conway, N. A. Crook, and M. W. Moncrieff, 1990: The generation and propagation of a nocturnal squall line. Part I: Observations and implications for mesoscale predictability. *Mon. Wea. Rev.,* **118,** 26–49.

——, J. W. Wilson, T. D. Keenan, and J. M. Hacker, 2000: Tropical island convection in the absence of significant topography. Part I: Life cycle of diurnally forced convection. *Mon. Wea. Rev.,* **128,** 3459–3480.

——, J. D. Tuttle, D. A. Ahijevych, and S. B. Trier, 2002: Inferences of predictability associated with warm season precipitation episodes. *J. Atmos. Sci.,* **59,** 2033–2056.

Carlson, T. N., and F. H. Ludlam, 1968: Conditions for the occurrence of severe local storms. *Tellus,* **20,** 203–226.

——, S. G. Benjamin, G. S. Forbes, and Y.-F. Lin, 1983: Elevated mixed layers in the regional severe storm environment: Conceptual model and case studies. *Mon. Wea. Rev.,* **111,** 1453–1474.

Charba, J., 1974: Application of gravity current model to analysis of squall-line gust front. *Mon. Wea. Rev.,* **102,** 140–156.

Childs, P. P., A. L. Qureshi, S. Raman, K. Alapaty, R. Ellis, R. Boyles, and D. Niyogi, 2006: Simulation of convective initiation during IHOP_2002 using the Flux-Adjusting Surface Data Assimilation System (FASDAS). *Mon Wea. Rev.,* **134,** 134–148.

Christian, T. W., and R. M. Wakimoto, 1989: The relationship between radar reflectivities and clouds associated with horizontal roll convection on 8 August 1982. *Mon. Wea. Rev.,* **117,** 1530–1544.

Christie, D. R., K. J. Muirhead, and A. L. Hales, 1979: Intrusive density flows in the lower troposphere: A source of atmospheric solitons. *J. Geophys. Res.,* **84,** 4959–4970.

Ciesielski, P. E., R. H. Johnson, P. T. Haertel, and J. Wang, 2003: Corrected TOGA COARE sounding humidity data: Impact on diagnosed properties of convection and climate over the warm pool. *J. Climate,* **16,** 2370–2384.

Crawford, T. M., and H. B. Bluestein, 1997: Characteristics of dryline passage during COPS-91. *Mon. Wea. Rev.,* **125,** 463–477.

Crook, N. A., 1996: Sensitivity of moist convection forced by boundary layer processes to low-level thermodynamic fields. *Mon. Wea. Rev.,* **124,** 1768–1785.

——, T. L. Clark, and M. W. Moncrieff, 1991: The Denver Cyclone. Part II: Interaction with the convective boundary layer. *J. Atmos. Sci.,* **48,** 2109–2126.

Dabberdt, W. F., and T. W. Schlatter, 1996: Research opportunities from emerging atmospheric observing and modeling capabilities. *Bull. Amer. Meteor. Soc.,* **77,** 305–323.

Dailey, P. S., and R. G. Fovell, 1999: Numerical simulation of the interaction between the sea-breeze front and horizontal convective rolls. Part I: Offshore ambient flow. *Mon. Wea. Rev.,* **127,** 858–878.

Demoz, B., and Coauthors, 2006: The dryline on 22 May 2002 during IHOP_2002: Convective–scale measurements at the profiling site. *Mon Wea. Rev.,* **134,** 294–310.

Dorien, P. B., S. Koch, and W. C. Skillman, 1988: The relationship between satellite-inferred frontogenesis and squall line formation. *Wea. Forecasting,* **3,** 319–342.

Doswell, C. A., III, 1987: The distinction between large-scale and mesoscale contribution to severe convection: A case study example. *Wea. Forecasting,* **2,** 3–16.

Doviak, R. J., and R. Ge, 1984: An atmospheric solitary gust observed with a Doppler radar, a tall tower and a surface network. *J. Atmos. Sci.,* **41,** 2559–2573.

——, S. S. Chen, and D. R. Christie, 1991: A thunderstorm-generated solitary wave observation compared with theory for nonlinear waves in a sheared atmosphere. *J. Atmos. Sci.,* **48,** 87–111.

Droegemeier, K. K., and R. B. Wilhelmson, 1985: Three-dimensional numerical modeling of convection produced by interacting thunderstorm outflows. Part I: Control simulation and low-level moisture variation. *J. Atmos. Sci.,* **42,** 2381–2403.

Emanuel, K., and Coauthors, 1995: Report of first prospectus development team of the U.S. weather research program to

NOAA and the NSF. *Bull. Amer. Meteor. Soc.,* **76,** 1194–1208.

Fabry, F., 2004: Meteorological value of ground target measurements by radar. *J. Atmos. Oceanic Technol.,* **21,** 591–604.

——, 2006: The spatial variability of moisture in the boundary layer and its effect on convection initiation: Project-long characterization. *Mon Wea. Rev.,* **134,** 79–91.

——, C. Frush, I. Zawadzki, and A. Kilambi, 1997: On the extraction of near-surface index of refraction using radar phase measurements from ground targets. *J. Atmos. Oceanic Technol.,* **14,** 978–987.

Fankhauser, J. C., N. A. Crook, J. Tuttle, L. J. Miller, and C. G. Wade, 1995: Initiation of deep convection along boundary layer convergence lines in a semitropical environment. *Mon. Wea. Rev.,* **123,** 291–313.

Fovell, R. G., and P. S. Dailey, 2001: Numerical simulation of the interaction between the sea-breeze front and horizontal convective rolls. Part II: Alongshore ambient flow. *Mon. Wea. Rev.,* **129,** 2057–2072.

Fritsch, J. M., and R. E. Carbone, 2004: Improving quantitative precipitation forecasts in the warm season: A USWRP research and development strategy. *Bull. Amer. Meteor. Soc.,* **85,** 955–966.

Fulton, R., D. S. Zrnic, and R. J. Doviak, 1990: Initiation of a solitary wave family in the demise of a nocturnal thunderstorm density current. *J. Atmos. Sci.,* **47,** 319–337.

Garstang, M., and H. J. Cooper, 1981: The role of near surface outflow in maintaining convective activity. *Proc. Nowcasting-I Symp.*, Copenhagen, Denmark, European Space Agency, 161–168.

Geerts, B., and R. Damiani, 2006: Finescale vertical structure of a cold front as revealed by an airborne Doppler radar. *Mon Wea. Rev.,* **134,** 251–271.

Goff, R. C., 1976: Vertical structure of thunderstorm outflows. *Mon. Wea. Rev.,* **104,** 1429–1440.

Grossman, R. L., 1982: An analysis of vertical velocity spectra obtained in the BOMEX fair-weather, trade-wind boundary layer. *Bound.-Layer Meteor.,* **23,** 323–357.

Guichard, F., D. Parsons, and E. Miller, 2000: Thermodynamic and radiative impact of the correction of sounding humidity bias in the tropics. *J. Climate,* **13,** 3611–3624.

Haase, S. P., and R. K. Smith, 1984: Morning glory wave clouds in Oklahoma: A case study. *Mon. Wea. Rev.,* **112,** 2078–2089.

Hane, C. E., C. J. Kessinger, and P. S. Ray, 1987: The Oklahoma squall line of 19 May 1977. Part II: Mechanisms for maintenance of the region of strong convection. *J. Atmos. Sci.,* **44,** 2866–2886.

——, C. L. Ziegler, and H. B. Bluestein, 1993: Investigation of the dryline and convective storms initiated along the dryline: Field experiments during COPS-91. *Bull. Amer. Meteor. Soc.,* **74,** 2133–2145.

——, H. B. Bluesein, T. M. Crawford, M. E. Baldwin, and R. M. Rabin, 1997: Severe thunderstorm development in relation to along-dryline variability: A case study. *Mon. Wea. Rev.,* **125,** 231–251.

——, M. E. Baldwin, H. B. Bluestein, T. M. Crawford, and R. M. Rabin, 2001: A case study of severe storm development along a dryline within a synoptically active environment. Part I: Dryline motion and an Eta Model forecast. *Mon. Wea. Rev.,* **129,** 2183–2204.

——, R. M. Rabin, T. M. Crawford, H. B. Bluestein, and M. E. Baldwin, 2002: A case study of severe storm development along a dryline within a synoptically active environment. Part II: Multiple boundaries and convection initiation. *Mon. Wea. Rev.,* **130,** 900–920.

Hill, K., G. S. Wilson, and R. E. Turner, 1979: NASA's participation in the AVE-SESAME '79 program. *Bull. Amer. Meteor. Soc.,* **60,** 1323–1329.

Hobbs, P. V., and P. O. G. Persson, 1982: The mesocale and microscale structure and organization of clouds and precipitation in midlatitude cyclones. Part V: The substructure of narrow cold-frontal rainbands. *J. Atmos. Sci.,* **39,** 280–295.

Holt, T. R., D. Niyogi, F. Chen, K. Manning, M. A. LeMone, and A. Qureshi, 2006: Effect of land–atmosphere interactions on the IHOP 24–25 May 2002 convection case. *Mon Wea. Rev.,* **134,** 113–133.

Intrieri, J. M., A. J. Bedard, and R. M. Hardesty, 1990: Details of colliding thunderstorm outflows as observed by Doppler lidar. *J. Atmos. Sci.,* **47,** 1081–1098.

Jorgensen, D. P., and T. M. Weckwerth, 2003: Forcing and organization of convective systems. *Radar and Atmospheric Science: A Collection of Essays in Honor of David Atlas*, R. M. Wakimoto and R. C. Srivastava, Eds., Amer. Meteor. Soc., 75–104.

Karan, H., and K. Knupp, 2006: Mobile Integrated Profiler System (MIPS) observations of low-level convergent boundaries during IHOP. *Mon. Wea. Rev.,* **134,** 92–112.

Karyampudi, V. M., S. E. Koch, J. W. Rottman, and M. L. Kaplan, 1995: The influence of the Rocky Mountains in the 13–14 April 1986 severe weather outbreak. Part II: Evolution of an internal bore and its role in triggering a squall line. *Mon. Wea. Rev.,* **123,** 1423–1446.

Kessinger, C. J., and C. K. Mueller, 1991: Background studies and nowcasting Florida thunderstorm activity in preparation for the CaPOW forecast experiment. Preprints, *25th Conf. on Radar Meteorology*, Paris, France, Amer. Meteor. Soc., 67–70.

Keyser, D., and M. A. Shapiro, 1986: A review of the structure and dynamics of upper-level frontal zones. *Mon. Wea. Rev.,* **114,** 452–499.

Kingsmill, D. E., 1995: Convection initiation associated with a sea-breeze front, a gust front, and their collision. *Mon. Wea. Rev.,* **123,** 2913–2933.

——, and N. A. Crook, 2003: An observational study of atmospheric bore formation from colliding density currents. *Mon. Wea. Rev.,* **131,** 2985–3002.

Knupp, K. R., B. Geerts, and S. J. Goodman, 1998: Analysis of a small, vigorous mesoscale convective system in a low-shear environment. Part I: Formation, radar echo structure, and lightning behavior. *Mon. Wea. Rev.,* **126,** 1812–1836.

Koch, S. E., 1984: The role of an apparent mesoscale frontogenetic circulation in squall line initiation. *Mon. Wea. Rev.,* **112,** 2090–2111.

——, and J. McCarthy, 1982: The evolution of an Oklahoma dryline. Part II: Boundary layer forcing of mesoconvective systems. *J. Atmos. Sci.,* **39,** 237–257.

——, and P. J. Kocin, 1991: Frontal contraction processes leading to the formation of an intense narrow rainband. *Meteor. Atmos. Phys.,* **46,** 123–154.

——, and W. L. Clark, 1999: A nonclassical cold front observed during COPS-91: Frontal structure and the process of severe storm initiation. *J. Atmos. Sci.,* **56,** 2862–2890.

——, P. B. Dorian, R. Ferrare, S. H. Melfi, W. C. Skillman, and D. Whiteman, 1991: Structure of an internal bore and dissipating gravity current as revealed by Raman lidar. *Mon. Wea. Rev.,* **119,** 857–887.

——, F. Zhang, M. L. Kaplan, Y.-L. Lin, R. Weglarz, and C. M. Trexler, 2001: Numerical simulations of a gravity wave event over CCOPE. Part III: The role of a mountain–plains solenoid in the generation of the second wave episode. *Mon. Wea. Rev.,* **129,** 909–933.

Kruse, F., III, and J. Johnson, 1995: Operational observation of a cold front and undular bore/gravity wave by 404 MHz wind profilers and the WSR-88D. Preprints, *27th Conf. on Radar Meteorology*, Vail, CO, Amer. Meteor. Soc., 163–166.

Kuettner, J. P., 1959: The band structure of the atmosphere. *Tellus,* **11,** 267–294.

——, 1971: Cloud bands in the earth's atmosphere. *Tellus,* **23,** 404–425.

Laird, N. F., D. A. R. Kristovich, R. M. Rauber, H. T. Ochs, and L. J. Miller, 1995: The Cape Canaveral sea and river breezes: Kinematic structure and convective initiation. *Mon. Wea. Rev.,* **123,** 2942–2956.

Langland, R. H., and Coauthors, 1999: The North Pacific Experiment (NORPEX-98): Targeted observations for improved North American weather forecasts. *Bull. Amer. Meteor. Soc.,* **80,** 1363–1384.

Lanicci, J. M., T. N. Carlson, and T. T. Warner, 1987: Sensitivity of the Great Plains severe-storm environment to soil-moisture distributions. *Mon. Wea. Rev.,* **115,** 2660–2673.

Lee, B. D., and R. B. Wilhelmson, 1997: The numerical simulation of non-supercell tornadogenesis. Part I: Initiation and evolution of pretornadic misocyclone circulations along a dry outflow boundary. *J. Atmos. Sci.,* **54,** 32–60.

——, R. D. Farley, and M. R. Hjelmfelt, 1991: A numerical case study of convection initiation along colliding convergence boundaries in northeast Colorado. *J. Atmos. Sci.,* **48,** 2350–2366.

LeMone, M. A., 1973: The structure and dynamics of horizontal roll vortices in the planetary boundary layer. *J. Atmos. Sci.,* **30,** 1077–1091.

——, and W. T. Pennell, 1976: The relationship of trade wind cumulus distribution to subcloud layer fluxes and structure. *Mon. Wea. Rev.,* **104,** 524–539.

——, G. M. Barnes, J. C. Fankhauser, and L. F. Tarleton, 1988: Perturbation pressure fields measured by aircraft around the cloud-base updraft of deep convective clouds. *Mon. Wea. Rev.,* **116,** 313–327.

——, E. Zipser, and S. B. Trier, 1998: The role of environmental shear and thermodynamic conditions in determining the structure and evolution of mesoscale convective systems during TOGA COARE. *J. Atmos. Sci.,* **55,** 3493–3518.

Locatelli, J. D., M. T. Stoelinga, P. V. Hobbs, and J. Johnson, 1998: Structure and evolution of an undular bore on the high plains and its effects on migrating birds. *Bull. Amer. Meteor. Soc.,* **79,** 1043–1060.

——, ——, and ——, 2002: A new look at the super outbreak of tornadoes on 3–4 April 1974. *Mon. Wea. Rev.,* **130,** 1633–1651.

Mahapatra, P. R., R. J. Doviak, and D. S. Zrnic, 1991: Multisensor observation of an atmospheric undular bore. *Bull. Amer. Meteor. Soc.,* **72,** 1468–1480.

Mahoney, W. P., 1988: Gust front characteristics and the kinematics associated with interacting thunderstorm outflows. *Mon. Wea. Rev.,* **116,** 1474–1491.

Markowski, P., and C. Hannon, 2006: Multiple-Doppler radar observations of the evolution of vorticity extrema in a convective boundary layer. *Mon Wea. Rev.,* **134,** 355–374.

——, ——, and E. Rasmussen, 2006: Observations of convection initiation "failure" from the 12 June 2002 IHOP deployment. *Mon Wea. Rev.,* **134,** 375–405.

Martin, W. J., and M. Xue, 2006: Sensitivity analysis of convection of the 24 May 2002 IHOP case using very large ensembles. *Mon Wea. Rev.,* **134,** 192–207.

May, P. T., 1999: Thermodynamic and vertical velocity structure of two gust fronts observed with a wind profiler/RASS during MCTEX. *Mon. Wea. Rev.,* **127,** 1796–1807.

McCarthy, J., and S. E. Koch, 1982: The evolution of an Oklahoma dryline. Part I: A mesoscale and subsynoptic-scale analysis. *J. Atmos. Sci.,* **39,** 225–236.

Mecikalski, J. R., and K. M. Bedka, 2006: Forecasting convective initiation by monitoring the evolution of moving cumulus in daytime GOES imagery. *Mon Wea. Rev.,* **134,** 49–78.

Menhofer, A., R. K. Smith, M. J. Reeder, and D. R. Christie, 1997: "Morning-glory" disturbances and the environment in which they propagate. *J. Atmos. Sci.,* **54,** 1712–1725.

Miller, R. C., 1959: Tornado-producing synoptic patterns. *Bull. Amer. Meteor. Soc.,* **40,** 465–472.

Moncrieff, M. W., and M. J. Miller, 1976: The dynamics and simulation of tropical cumulonimbus and squall lines. *Quart. J. Roy. Meteor. Soc.,* **102,** 373–394.

Mueller, C. K., and R. E. Carbone, 1987: Dynamics of a thunderstorm outflow. *J. Atmos. Sci.,* **44,** 1879–1898.

Murphey, H. V., R. M. Wakimoto, C. Flamant, and D. E. Kingsmill, 2006: Dryline on 19 June 2002 during IHOP. Part I: Airborne Doppler and LEANDRE II analyses of the thin line structure and convection initiation. *Mon Wea. Rev.,* **134,** 406–430.

National Research Council, 1998: *The Atmospheric Sciences: Entering the Twenty-First Century*. National Academy Press, 364 pp.

Neiman, P. J., and R. M. Wakimoto, 1999: The interaction of a Pacific cold front with shallow air masses east of the Rocky Mountains. *Mon. Wea. Rev.,* **127,** 2102–2127.

Newton, C. W., 1963: Dynamics of severe convective storms. *Severe Convective Storms, Meteor. Monogr.*, No. 27, Amer. Meteor. Soc., 33–58.

NSSP Staff, 1963: Environmental and thunderstorm structures as shown by the National Severe Storms Project observations in spring 1960 and 1961. *Mon. Wea. Rev.,* **91,** 1671–1681.

Ogura, Y., 1982: Possible triggering mechanisms for severe storms in SESAME-AVE IV (9–10 May 1979). *Bull. Amer. Meteor. Soc.,* **63,** 503–515.

Parsons, D. B., 1992: An explanation for intense frontal updrafts and narrow cold-frontal rainbands. *J. Atmos. Sci.,* **49,** 1810–1825.

——, and P. V. Hobbs, 1983: The mesoscale and microscale structure and organization of clouds and precipitation in midlatitude cyclones. Part XI: Comparisons between observational and theoretical aspects of rainbands. *J. Atmos. Sci.,* **40,** 2377–2398.

——, M. A. Shapiro, R. M. Hardesty, R. J. Zamora, and J. M. Intrieri, 1991: The finescale structure of a west Texas dryline. *Mon. Wea. Rev.,* **119,** 1242–1258.

——, ——, and E. Miller, 2000: The mesoscale structure of a nocturnal dryline and of a frontal-dryline merger. *Mon. Wea. Rev.,* **128,** 3824–3838.

Purdom, J. F. W., 1982: Subjective interpretations of geostationary satellite data for nowcasting. *Nowcasting*, K. Browning, Ed., Academic Press, 149–166.

——, and K. Marcus, 1982: Thunderstorm trigger mechanisms over the southeast U.S. Preprints, *12th Conf. on Severe Local Storms*, San Antonio, TX, Amer. Meteor. Soc., 487–488.

Raymond, D. J., 1995: Regulation of moist convection over the west Pacific warm pool. *J. Atmos. Sci.,* **52,** 3945–3959.

Reed, R. J., and M. D. Albright, 1997: Frontal structure in the interior of an intense mature ocean cyclone. *Wea. Forecasting,* **12,** 866–876.

Reinking, R. F., R. J. Doviak, and R. O. Gilmer, 1981: Clear-air roll vortices and turbulent motions as detected with an airborne gust probe and dual-Doppler radar. *J. Appl. Meteor.,* **20,** 678–685.

Revercomb, H. E., and Coauthors, 2003: The ARM Program's water vapor intensive observation periods. *Bull. Amer. Meteor. Soc.,* **84,** 217–236.

Rhea, J. O., 1966: A study of thunderstorm formation along drylines. *J. Appl. Meteor.,* **5,** 58–63.

Roberts, R. D., and S. Rutledge, 2003: Nowcasting storm initiation and growth using *GOES-8* and WSR-88D data. *Wea. Forecasting,* **18,** 562–584.

Rotunno, R., J. B. Klemp, and M. L. Weisman, 1988: A theory for strong, long-lived squall lines. *J. Atmos. Sci.,* **45,** 463–485.

Sanders, F., and D. O. Blanchard, 1993: The origin of a severe thunderstorm in Kansas on 10 May 1985. *Mon. Wea. Rev.,* **121,** 133–149.

Schaefer, J. T., 1986: The dryline. *Mesoscale Meteorology and Forecasting*, P. S. Ray, Ed., Amer. Meteor. Soc., 549–572.

Segal, M., and R. W. Arritt, 1992: Nonclassical mesoscale circulations caused by surface sensible heat-flux gradients. *Bull. Amer. Meteor. Soc.,* **73,** 1593–1604.

Seitter, K. L., 1986: A numerical study of atmospheric density current motion including the effect of condensation. *J. Atmos. Sci.,* **43,** 3068–3076.

Shapiro, M. A., 1981: Frontogenesis and geostrophically forced secondary circulations in the vicinity of jet streams–frontal zone systems. *J. Atmos. Sci.,* **38,** 954–973.

——, 1982: Mesoscale weather systems of the central United States. CIRES, 78 pp. [Available from Cooperative Institute for Research in Environmental Sciences (CIRES), Boulder, CO 80309.]

——, T. Hampel, D. Rotzoll, and F. Mosher, 1985: The frontal hydralic head: A micro-alpha scale (~1 km) triggering mechanism for mesoconvective weather systems. *Mon. Wea. Rev.,* **113,** 1166–1183.

Shreffler, J. H., and F. S. Binkowski, 1981: Observations of pressure jump lines in the Midwest, 10–12 August 1976. *Mon. Wea. Rev.,* **109,** 1713–1725.

Skyllingstad, E. D., 1991: Critical layer effects on atmospheric solitary and cnoidal waves. *J. Atmos. Sci.,* **48,** 1613–1624.

Soden, B., and J. Lanzante, 1996: An assessment of satellite and radiosonde climatologies of upper-tropospheric water vapor. *J. Climate,* **9,** 1235–1250.

Soong, S. T., and W. K. Tao, 1984: A numerical study of the vertical transport of momentum in a tropical rainband. *J. Atmos. Sci.,* **41,** 1049–1061.

Stensrud, D. J., and R. A. Maddox, 1988: Opposing mesoscale circulations: A case study. *Wea. Forecasting,* **3,** 189–204.

——, and J. M. Fritsch, 1994: Mesoscale convective systems in weakly forced large-scale environments. Part II: Generation of mesoscale initiation condition. *Mon. Wea. Rev.,* **122,** 2068–2083.

——, G. S. Manikin, E. Rogers, and K. E. Mitchell, 1999: Importance of cold pools to NCEP mesoscale Eta Model forecasts. *Wea. Forecasting,* **14,** 650–670.

Sun, W.-Y., and C.-C. Wu, 1992: Formation and diurnal variation of the dryline. *J. Atmos. Sci.,* **49,** 1606–1619.

Tegtmeier, S. A., 1974: The role of the surface, sub-synoptic, low pressure system in severe weather forecasting. M.S. thesis, School of Meteorology, University of Oklahoma, Norman, 66 pp.

Tepper, M., 1950: A proposed mechanism of squall lines—The pressure jump line. *J. Meteor.,* **7,** 21–29.

Trier, S. B., D. B. Parsons, and J. H. E. Clark, 1991: Environment and evolution of a cold-frontal mesoscale convective system. *Mon. Wea. Rev.,* **119,** 2429–2455.

Turner, D. D., B. M. Lesht, S. A. Clough, J. C. Liljegren, H. E. Revercomb, and D. C. Tobin, 2003: Dry bias and variability in Vaisala radiosondes: The ARM experience. *J. Atmos. Oceanic Technol.,* **20,** 117–132.

Uccellini, L. W., and D. R. Johnson, 1979: The coupling of upper and lower tropospheric jet streaks and implications for the development of severe convective storms. *Mon. Wea. Rev.,* **107,** 682–703.

——, P. J. Kocin, and J. M. Sienkiewicz, 1999: Advances in forecasting extratropical cyclogenesis at the National Meteorological Center. *The Life Cycles of Extratropical Cyclones,* M. A. Shapiro and S. Grønås, Eds., Amer. Meteor. Soc., 317–336.

Ulanski, S. L., and M. Garstang, 1978: The role of surface divergence and vorticity in the life cycle of convective rainfall. Part I: Observations and analysis. *J. Atmos. Sci.,* **35,** 1047–1062.

Wakimoto, R. M., 1982: The life cycle of thunderstorm gust fronts as viewed with Doppler radar and rawinsonde data. *Mon. Wea. Rev.,* **110,** 1060–1082.

——, and J. W. Wilson, 1989: Nonsupercell tornadoes. *Mon. Wea. Rev.,* **117,** 1113–1140.

——, and N. T. Atkins, 1994: Observations of the sea-breeze front during CaPE. Part I: Single-Doppler, satellite, and cloud photogrammetric analysis. *Mon. Wea. Rev.,* **122,** 1092–1114.

——, and J. K. Lew, 1993: Observations of a Florida waterspout during CaPE. *Wea. Forecasting,* **8,** 412–423.

——, and D. E. Kingsmill, 1995: Structure of an atmospheric undular bore generated from colliding boundaries during CaPE. *Mon. Wea. Rev.,* **123,** 1374–1393.

——, H. V. Murphey, E. V. Browell, and S. Ismail, 2006: The "triple point" on 24 May 2002 during IHOP. Part I: Airborne Doppler and LASE analyses of the frontal boundaries and convection initiation. *Mon Wea. Rev.,* **134,** 231–250.

Wallace, J. M., 1975: Diurnal variations in precipitation and thunderstorm frequency over the conterminous United States. *Mon. Wea. Rev.,* **103,** 406–419.

Wang, J., H. L. Cole, D. J. Carlson, E. R. Miller, K. Beierle, A. Paukkunen, and T. K. Laine, 2002: Corrections of humidity measurement errors from the Vaisala RS80 radiosonde—Application to TOGA_COARE data. *J. Atmos. Oceanic Technol.,* **19,** 981–1002.

——, D. J. Carlson, D. B. Parsons, T. F. Hock, D. Lauritsen, H. L. Cole, K. Beierle, and E. Chamberlain, 2003: Performance of operational radiosonde humidity sensors in direct comparison with a chilled mirror dew-point hygrometer and its climate implication. *Geophys. Res. Lett.,* **30,** 1860, doi:10.1029/2003GL016985.

Watson, I. W., and D. O. Blanchard, 1984: The relationship between total area divergence and convective precipitation in south Florida. *Mon. Wea. Rev.,* **112,** 673–685.

Weaver, J. F., D. Lindsey, D. Bikos, C. C. Schmidt, and E. Prins, 2004: Fire weather detection using GOES rapid scan imagery. *Wea. Forcasting,* **19,** 496–510.

Weckwerth, T. M., 2000: The effect of small-scale moisture variability on thunderstorm initiation. *Mon. Wea. Rev.,* **128,** 4017–4030.

——, and R. M. Wakimoto, 1992: The initiation and organization of convective cells atop a cold-air outflow boundary. *Mon. Wea. Rev.,* **120,** 2169–2187.

——, J. W. Wilson, and R. M. Wakimoto, 1996: Thermodynamic variability within the convective boundary layer due to horizontal convective rolls. *Mon. Wea. Rev.,* **124,** 769–784.

——, ——, ——, and N. A. Crook, 1997: Horizontal convective rolls: Determining the environmental conditions supporting their existence and characteristics. *Mon. Wea. Rev.,* **125,** 505–526.

——, V. Wulfmeyer, R. M. Wakimoto, R. M. Hardesty, J. W. Wilson, and R. M. Banta, 1999: NCAR–NOAA lower-tropospheric water vapor workshop. *Bull. Amer. Meteor. Soc.,* **80,** 2339–2357.

——, and Coauthors, 2004: An overview of the International H_2O Project (IHOP_2002) and some preliminary highlights. *Bull. Amer. Meteor. Soc.,* **85,** 253–277.

——, C. R. Pettet, F. Fabry, S. Park, M. A. LeMone, and J. W. Wilson, 2005: Radar refractivity retrieval: Validation and application to short-term forecasting. *J. Appl. Meteor.,* **44,** 285–300.

Weiss, C. C., and H. B. Bluestein, 2002: Airborne pseudo-dual-Doppler analysis of a dryline–outflow boundary intersection. *Mon. Wea. Rev.,* **130,** 1207–1226.

——, ——, and A. L. Pazmany, 2006: Finescale radar observations of the 22 May 2002 dryline during the International H_2O Project (IHOP). *Mon Wea. Rev.,* **134,** 273–293.

Wilson, J. W., and W. E. Schreiber, 1986: Initiation of convective storms at radar-observed boundary-layer convergence lines. *Mon. Wea. Rev.,* **114,** 2516–2536.

——, and C. K. Mueller, 1993: Nowcasts of thunderstorm initiation and evolution. *Wea. Forecasting,* **8,** 113–131.

——, and D. L. Megenhardt, 1997: Thunderstorm initiation, organization and lifetime associated with Florida boundary layer convergence lines. *Mon. Wea. Rev.,* **125,** 1507–1525.

——, and R. D. Roberts, 2006: Summary of convective storm initiation and evolution during IHOP: Observational and modeling perspective. *Mon Wea. Rev.,* **134,** 23–47.

——, G. B. Foote, N. A. Crook, J. C. Fankhauser, C. G. Wade, J. D. Tuttle, C. K. Mueller, and S. K. Krueger, 1992: The role of boundary-layer convergence zones and horizontal rolls in the initiation of thunderstorms: A case study. *Mon. Wea. Rev.,* **120,** 1785–1815.

——, T. M. Weckwerth, J. Vivekanandan, R. M. Wakimoto, and R. W. Russell, 1994: Boundary layer clear-air radar echoes: Origin of echoes and accuracy of derived winds. *J. Atmos. Oceanic Technol.,* **11,** 1184–1206.

——, N. A. Crook, C. K. Mueller, J. Sun, and M. Dixon, 1998: Nowcasting thunderstorms: A status report. *Bull. Amer. Meteor. Soc.,* **79,** 2079–2100.

Wulfmeyer, V., H.-S. Bauer, M. Grzeschik, A. Behrendt, F. Vandenberghe, E. V. Browell, S. Ismail, and R. A. Ferrare, 2006: Four-dimensional variational assimilation of water vapor differential absorption lidar data: The first cast study within IHOP_2002. *Mon Wea. Rev.,* **134,** 209–230.

Xue, M., and W. J. Martin, 2006a: A high-resolution modeling study of the 24 May 2002 dryline case during IHOP. Part I: Numerical simulation and general evolution of the dryline and convection. *Mon Wea. Rev.,* **134,** 149–171.

——, and ——, 2006b: A high-resolution modeling study of the 24 May 2002 dryline case during IHOP. Part II: Horizontal convective rolls and convective initiation. *Mon Wea. Rev.,* **134,** 172–191.

Ziegler, C. L., and E. N. Rasmussen, 1998: The initiation of moist convection at the dryline: Forecasting issues from a case study perspective. *Wea. Forecasting,* **13,** 1106–1131.

——, T. J. Lee, and R. A. Pielke Sr., 1997: Convection initiation at the dryline: A modeling study. *Mon. Wea. Rev.,* **125,** 1001–1026.

——, D. Kennedy, and E. N. Rasmussen, 2004: A wireless network for collection and synthesis of mobile mesoscale weather observations. *J. Atmos. Oceanic Technol.,* **21,** 1659–1670.